SHOCK DEFORMATION OF INCONEL 600 ALLOY: EFFECT OF FINE COHERENT PRECIPITATES ON EXPLOSIVE-SHOCK HARDENING

N69-75807

L. E. Murr
Departments of Materials Science
and Electrical Engineering
University of Southern California
Los Angeles, California 90007

and

J. V. Foltz
Ballistics Division
U.S. Naval Weapons Laboratory
Dahlgren, Virginia 22448

ABSTRACT

Sheet samples of pure nickel and Inconel 600 alloy (76% Ni, 16% Cr, 7% Fe) containing a fine precipitate were simultaneously shock-loaded in sandwich assemblies at pressures of 50, 100, 150, 200 and 370 kilobars by a planar pulse of roughly 2 microseconds duration explosively initiated by a flying plate. The residual microhardness of the nickel was observed to saturate above about 300 Kb while that for Inconel continued to increase steadily. Examination of the nickel substructures by transmission electron microscopy revealed a steadily decreasing cell size with increasing shock pressure; with almost no evidence of deformation twins at 370 Kb. The Inconel substructure was characterized by planar dislocation arrays which included an increasing concentration of dipoles and elongated loops to 200 Kb; while at 370 Kb deformation twins having an average thickness of 150 Å and occupying 19% of the volume were observed. The coherent precipitates in the Inconel matrix were observed to become incoherent at pressures above 50 Kb, with the concommitent production of dislocation tangles and loops at the particle-matrix interface. The precipitates were observed to enhance shock hardening by acting as sources for dislocation dipoles and elongated loops.

1. INTRODUCTION

In the decade since the original metallurgical investigations of the residual properties of shock deformed solids [1], a considerable body of information has been amassed concerning the response of metals and alloys to the passage of a planar shock wave. In particular, the shock induced defect structures of a number of materials have been studied by transmission electron microscopy and correlated with residual mechanical properties [2-11]. Among other things, it now appears that relative stacking-fault free energy is an effective parameter for characterizing residual shock-defect microstructures; and this is particularly true for very low stacking-fault energy materials ($\gamma_{SF} \tilde{=}$ 2-25 ergs/cm^2).

It is generally thought that dislocations originate at sources randomly disposed within the grains of polycrystalline materials, in addition to the grain boundaries. Thus, the shock wave profile will depend upon the number of such sources, the mobility of existing dislocations, the spacings of these mobile dislocations, and their velocities; and will be effectively regulated by the pressure and temperature dependence of the elastic constants of the material. In low stacking-fault energy FCC materials, dislocations are unable, for the most part, to cross-slip. The residual defect microstructures in these materials are therefore characterized by planar dislocation arrays, stacking-faults, and imperfectly formed microtwins. Conversely, high stacking-fault energy materials exhibit varying degrees of dislocation cell struct-

ures following shock deformation as a result of extensive cross-slip.

Since the residual hardness of a solid is influenced primarily by defect character, density, and spatial arrangement; it is expected that with the introduction of more or different defects, the hardness will be altered. Above all, we find that retardation of dislocation mobility by jogs, point defect pinning, microstructural barriers such as planar interfaces, or inclusions is primarily responsible for the work hardening of solids [12].

On considering that there have been no reported experiments specifically designed to investigate the effects of matrix inclusions on residual shock hardening, it was decided that such an investigation could contribute to our understanding of the general characterization of shock hardening. The present investigation therefore details the results gleaned from an investigation of the residual shock hardening in an alloy matrix containing coherent precipitates.

The objectives of the present investigation were first to study the systematic hardening with shock pressure of Inconel 600 alloy (76% Ni, 16% Cr, 7% Fe) containing fine, coherent precipitates; and to compare the residual hardening with that of pure nickel simultaneously shock-loaded in the same experiment using a technique devised by Grace [13]. Secondly, the direct observation and comparison of residual defect microstructures by transmission electron microscopy was intended to elucidate the hardening mechanisms in these materials of different stacking-fault free energy. Thirdly, it was desirable to study the response of coherent precipitates having large residual strain fields to shock wave passage, particularly with regard to the particle-matrix interface, the coherency of the inter-

face following shock attack, the generation of interfacial dislocations, and the ability of such inclusions to obstruct dislocation mobility or to act as dislocation sources.

2. EXPERIMENTAL PROCEDURE

Four sheet samples of Inconel 600 alloy (Table 1) (0.001 in. thick-annealed for 15 min. at 1060°C) were sandwiched between two sheet samples of pure nickel (Table 1) (0.004 in. thick-annealed for 15 min. at 1060°C); and this laminated arrangement pressed in a nickel sandwich assembly measuring 0.750 x 1.250 in. Five sandwich assemblies of this type were fabricated having an overall thickness of 0.500 in. with the specimen sheets positioned approximately 0.150 in. from the top or impact surface. These experimental sheet sandwiches were then explosively shock-loaded in the assembly arrangement sketched schematically in Fig. 1; using the procedures previously discussed by Rose and Grace[14]. In this arrangement, variation of the driver plate thickness and the explosive height allowed a desirable planar shock pressure to be attained[10], with the final pressures being determined for each experiment using shorting-pin switches to measure driver plate velocities. Pressures of 50, 100, 150, 200 and 370 Kilobars were obtained in the five experimental sandwich assemblies, with the shock-pulse duration maintained constant at approximately 2 microseconds.

On shock-loading the experimental assemblies (Fig. 1), the specimen sandwiches, still intact, were blown into a water recovery tank. These assemblies were then separated and the hardness of the nickel and Inconel sheet materials measured in a Vickers microhardness tester using a 50 gm load.

Specimens for transmission electron microscopy were prepared from 0.50 in. wide sections cut from the shock-loaded sheets employing the technique previously described by Murr[15]. Using an electrolyte consisting of 42% phosphoric acid, 34% sulfuric acid, 24% water; and a current density held constant at roughly 3 amp/cm^2, thin samples of Inconel could be prepared in roughly 5 min. while the nickel required from 5-15 min. Normally, the electron transparent areas corresponded to regions roughly centered in the sandwich geometry; and the foil surfaces were of course perpendicular to the direction of shock-wave propagation, and in the plane of the original sandwich sheets. Representative areas from numerous thin samples of each shock-loaded material and the initial (annealed) materials were observed and photographed in a Hitachi 125 electron microscope operated at 125 kV, and fitted with a universal tilting stage.

3. RESULTS

The results of Vickers microhardness measurements on the shock-loaded and annealed nickel and Inconel samples are shown in Fig. 2. Each

point plotted represents the average of 50 hardness indentations; 25 indentations per side of sample. It is apparent at first glance that considerably more hardening occurs in the Inconel than in pure nickel subjected simultaneously to the same shock pulse; and that the hardening characteristics are considerably different. The hardening curve for pure nickel shown in Fig. 2 exactly follows that obtained from data of Rose[16]; with the curve shifted by 50 hardness numbers to compensate for the difference in starting (annealed) sample hardness. It is observed that nickel, for the most part, has saturated in shock hardness between 200 and 300 Kilobars. The hardening of Inconel, on the other hand, rises steadily for pressures in excess of 100 Kb, and shows no sign of leveling off at 370 Kb.

Direct observation of the nickel and Inconel samples in the annealed (unshocked) state revealed an average grain size in each of 15-20 μ. The Inconel samples contained a distribution of coherent precipitates of the form M_xC which was, in most cases, not completely homogeneous within the grains. Figure 3 illustrates what might be identified as the typical precipitate distribution in the Inconel showing the characteristic coherency strain fields; and the approximate initial character and density of dislocations. It is to be noted that the precipitates have a tendency to segregate in slip planes.

Figure 4 shows the residual microstructure in the Inconel samples shock-loaded at 50 Kb. The precipitates are observed to have lost some

coherency as evidenced by the general lack of strain field contrast (Fig. 3 at "S"). Dislocations, particularly the ends of dipoles, are observed to be anchored at numerous precipitates; and there is considerable generation of elongated dislocation loops amongst the profusion of dislocation dipoles. This latter feature is particularly noticeable in Fig. 5 which shows for comparison another section of residual microstructure following shock-loading at 50 Kb.

Figure 5 illustrates quite clearly the production of jogs which trail dislocation dipoles as they are swept through the lattice presumably in the shock front. This is particularly noticeable in portions of Fig. 5 denoted by "dp". In most cases, loops having sometimes a predominant edge character have formed by the creation of dipoles on small jogs - at "p". These dislocation dipoles are formed by cross-slip of predominantly screw dislocations encountering the precipitates in their glide planes. This feature is evidenced by the occurrence of dipoles and loops in pairs or in greater numbers in Fig. 5 as discussed by Groves and Kelly[17]. Smaller loops observed in the immediate vicinity of the precipitates presumably result by prismatic punching[18] as the particles are strained incoherently from the matrix.

The substructural trend indicated in Figs. 4 and 5 was observed to continue at pressures of 100 and 150 Kb, with the precipitates becoming completely incoherent. The dipoles and associated loops appeared to be increasingly elongated with increasing shock pressure. Following 200 Kb

shock-loading, a profusion of dislocations, particularly the ends of dipoles were observed to be associated with the precipitates. Figure 6 illustrates the shock-induced defect structure following the passage of a 200 Kb shock pulse; and the reader will readily observe the distinct increase in dislocation density, particularly dipoles, compared with samples shock-loaded at 50 Kb as shown in Figs. 4 and 5.

It should also be observed in Figs. 4-6 that the dislocations are generally observed to occur in planar arrays (the dipoles are noticeably oriented in the slip plane) as opposed to the dislocation cell structures observed in pure nickel[2,16]; a feature generally indicative of a low stacking-fault energy material. Also consistent with shock-loading of low stacking-fault energy materials[4,8,11] was the onset of appreciable deformation twinning at 370 Kb in the Inconel as shown in Figs. 7 and 8. It was observed that measurement of the average twin widths at intersections such as those shown in Fig. 7 (at "i"); and crystallographic situations where the twins were normal to the specimen-grain surfaces, consistently produced a value of 150 Å. This is the same value observed for the widths of shock-induced deformation twins in brass and stainless steel[11].

By comparison, the residual defect structures in nickel simultaneously shock-loaded to 370 Kb were observed to be very small dislocation cells (having a mean diameter of approximately 0.17 μ) which appeared

to be breaking up into a more or less continuous dense distribution of dislocations. Figure 9 illustrates the typical appearance of the nickel substructure. Contrary to the claims of Nolder and Thomas[2], practically no evidence of deformation twinning was observed at 370 Kb in the nickel. The volume density of twinned material at this pressure was in fact much less than 0.1 percent. This result is also significantly less than that observed for x-ray diffraction by Rose[16]. Our results are, however, in general agreement with those of Nolder and Thomas[2] and Rose[16] in that in nickel, dislocation cell size is observed to decrease with increasing shock pressure in the range 0 - 350 Kb. It should also be noted that the cell size observed in nickel at 370 Kb is the upper limit of cell size range indicated by Nolder and Thomas[2] to be critical for the initiation of mechanical twins.

Table 2 illustrates the results of measurements of dislocation and twin volume density in the Inconel samples. The dislocation densities (including the dipoles) were measured by the technique of Ham[19] using square grid meshes so that in effect

$$\Lambda = 2N/Lt \qquad (1)$$

where N is the number of dislocation intersections for a total length of grid lines L; and a local specimen thickness of t. Dislocation densities were measured for each pressure as well as the annealed starting material from a series of micrographs, each possessing a strong low-order reflection.

The proportion of invisible dislocations was then accounted for by considering the suggestions of Hirsch and Steeds[20]. The total area of random thin sections included in each series of dislocation density measurements was always greater than 200 μ^2.

Twin volume densities (volume percent) measured in Inconel foils following shock-loading at 370 Kb were estimated from

$$\Lambda(T) = \overline{w_T} \cdot 10^2 \sum_j \left(\frac{L_j}{A_j \sin \theta} \right) \qquad (2)$$

where θ is the inclination of {111} fault planes with the crystallographic surface, L is the total twin length over an area A of foil; and $\overline{w_T}$ is the average twin width indicated previously to have been determined as 150 Å (Fig. 7). The volume density of twinned material in Inconel shock-loaded to 370 Kb was found to be roughly 19 percent.

The regular increases in dislocation densities after 50 Kb shock pressure as indicated in Table 2 are readily applicable to a cursory identification of the hardening trends shown in Fig. 2. It should also be noted that the hardening increase may be due to the energy contribution to work-hardening of the elongating dislocation loops, and the impedence to dislocation motion afforded by the long dislocation dipoles.

The contribution of the deformation twins in Inconel shock-loaded to 370 Kb to the residual hardening appears to result by the impedance to dislocation motion afforded by the twin boundaries. It is apparent from the

contrast featured in Fig. 8 that the twin boundaries contain a high density of dislocations. If these dislocations are primarily interfacial dislocations, i.e., at the twin-matrix interface, then the twins, as shown in Fig. 8, will function effectively in the same manner as grain boundaries in blocking dislocation motion, ie., by the formation of sub-grain domains. This feature may in fact be responsible in other shock-hardened materials where deformation twinning is observed to predominate[4, 8, 11].

The stabilization shock hardening in pure nickel shown in Fig. 2 can be understood in terms of dislocation saturation and cell densification above about 300 Kb as previously demonstrared by Nolder and Thomas[2], and Rose[21]. It appears that because of the nature of the residual defect structure (dislocation cells) as it is effectively regulated by stacking-fault energy; shock-loading of high stacking-fault energy materials is limited by a plateau region which exhibits some temperature dependence. In effect, shock-loading of these materials above about 500 Kb produces residual structures and hardness which tend to revert to the annealed condition because of shock heating effects. This same phonomenon also occurs in low stacking-fault energy materials[8].

4. DISCUSSION

On considering the results of the present investigation for shock-loading of Inconel 600 alloy containing precipitates, we can readily observe that the effect of such inclusions is to enhance the residual shock hardening by acting as new sources of dislocations - dislocation dipoles and elongated

loops. Measurement of the dislocation densities in an area 1 micron on a side surrounding individual precipitates (such as those observed in Figs. 5 and 6) indicated densities ranging up to three times that observed in the overall thin section. While there was no consistent trend, the generation of dislocations at precipitates appeared to be greatest at higher pressures, consistent with the increasing tendency to generate an incoherent interface resulting from the difference in compressibility and expansion between the particles and the alloy matrix. While it is possible that a difference in elastic constants of the particles and the Inconel matrix may have influenced the establishment of a particle-matrix interface, it appears more likely that the thermal properties associated with the shock front propagation caused a difference in the particle-matrix expansion; with the simultaneous production of prismatic dislocation loops or tangles during shock relief (rarefaction). In addition, dislocations generated elsewhere in the Inconel matrix, particularly grain boundaries, became entangled in the precipitates, sometimes causing new dislocation sources to be established; and aiding in the production of long dipoles and loops by the obstacle surmounting mechanism described previously. No evidence was found for particle shearing.

We might finally discuss the dislocation sources for twinning dislocations in the formation of deformation twins at 370 Kb in Inconel 600. Generally, most of the dislocation pole mechanisms have appeared inadequate

in explaining the high-rate twin formation in shock-loaded materials; and twinning in FCC materials of low stacking-fault energy have been ascribed to the pile-up of dislocations at an obstacle, and the subsequent dissociation into partials[4,10,11]. In Inconel 600, the occurrence of obstacles is enhanced by the precipitates, but the formation of partial dislocations has not been observed generally. This in itself is a somewhat peculiar behavior of Inconel since the stacking-fault energy has been measured to be approximately 24 ergs/cm^2 [22]; and this, of course, characterizes Inconel as a low stacking-fault energy material as compared with the concurrently investigated nickel, which has an approximate stacking-fault energy of about 300 ergs/cm^2 [23]. On the other hand, the profusion of dislocation dipoles in the residual Inconel substructures attests to the high probability of an abundance of undissociated superjogs which could act as nuclei for pole-twin sources as proposed by Venables[24]. The plausibility of this latter mechanism, in light of the present results, is now being pursued in detail.

5. CONCLUSIONS

The results of the present investigation allow the following conclusions to be drawn:

1. The effect of coherent precipitates on shock-hardening is to enhance the phenomenon by acting as sources for additional dislocations, dislocation dipoles and loops; as well as barriers to dislocation motion.

2. Coherent precipitates in Inconel become incoherent as the explosive shock pressure exceeds about 100 Kb with a concomitant production of prismatic dislocation loops and tangles at the particle-matrix interface.

3. The residual defect structures in shock-loaded Inconel are characterized by planar arrays of dislocations, dislocation dipoles, and dislocation loops; with the onset of deformation twinning occurring between 200 and 370 Kb.

4. Deformation twinning is not prominent in nickel at 370 Kb; and represents less than 0.1% of the volume density. Residual shock hardening in nickel occurs by a densification of dislocation cells with increasing shock pressure.

5. Twinning in planar shock-loaded materials is dependent to some degree upon the so-called "room temperature" stacking-fault energy and a critical shear stress which itself may be stacking-fault energy dependent. The onset of twinning is also temperature dependent; and thermal heating apparently places an upper limit on the shock-hardening in any material.

6. Residual hardening due to deformation twins can occur by the effective division of existing grains into sub-grain domains, with the twin boundaries acting as barriers to the motion of matrix glide dislocations.

ACKNOWLEDGMENTS

The authors are grateful to Dr. F. I. Grace for his contributions to the experimental efforts; and to Mr. R.J. Horylev for assisting in the experimental measurements. The shock loading was performed at the USNWL test facility and this portion of the research supported by a USNWL Foundational Research Program. Partial research support by the USC Joint Services Electronics Grant AF-AFOSR-496-67; and support of the major portions of this work by a NASA Multidisciplinary Research Grant NGL-05-018-044 is also gratefully acknowledged. This work was performed, for the most part, while one of us (J.V.F.) was a visiting research associate in the Materials Science Department at the University of Southern California.

REFERENCES

1. C. S. Smith, Trans. Met. Soc. AIME, 212, 574 (1958).
2. R. L. Nolder and G. Thomas, Acta Met., 12, 227 (1964).
3. O. Johari and G. Thomas, Acta Met., 12, 1153 (1964).
4. M. C. Inman, L. E. Murr, and M. F. Rose, Adv. Electron Metal. (ASTM), STP396, 39 (1966).
5. A. S. Iyer and P. Gordon, Trans. Met. Soc. AIME, 224, 1077 (1962).
6. D. C. Brillhart, R. J. DeAngelis, A. G. Preban, J. B. Cohen, and P. Gordon, Trans. Met. Soc. AIME, 239, 836 (1967).
7. A. S. Appleton and J. S. Waddington, Phil. Mag., 12, 273 (1965).
8. F. I. Grace, M. C. Inman and L. E. Murr, Brit. J. Appl. Phys., 1, 1437 (1968).
9. L. E. Murr and M. F. Rose, Phil. Mag., 18, 281 (1968).
10. L. E. Murr and F. I. Grace, Exp. Mchs. (SESA) April (1969).
11. L. E. Murr and F. I. Grace, unpublished.
12. J. Friedel, in Electron Microscopy and Strength of Crystals, Interscience Publishers, New York, (1963).
13. F. I. Grace, Ph. D. Dissertation, The Pennsylvania State University, University Park, Pa. (1967).
14. M. F. Rose and F. I. Grace, Brit. J. Appl. Phys., 18, 671 (1967).
15. L. E. Murr, Appl. Mater. Res., 3, 466 (1964).
16. M. F. Rose, Ph. D. Dissertation, The Pennsylvania State University, University Park, Pa. (1966).
17. G. W. Groves and A. Kelly, Proc. Roy. Soc., A275, 233 (1963).

18. D. H. Jones and J. W. Mitchell, Phil. Mag., 3, 1 (1958).

19. R. K. Ham, Phil. Mag., 6, 1183 (1961).

20. P. B. Hirsch and J. W. Steeds, Relation Between the Structure and Mechanical Properties of Metals, N. P. L. Symposium No. 15, p. 39 (1964; see also Table 17.1 of P. B. Hirsch, et al., Electron Microscopy of Thin Crystals, Butterworths, London, p. 423 (1965).

21. M. F. Rose, M. S. Thesis, The Pennsylvania State University, University Park, Pa. (1964).

22. L. E. Murr, unpublished.

23. T. Jøssang and J. P. Hirth, Phil. Mag., 13, 657 (1966).

24. J. A. Venables, Phil. Mag., 6, 379 (1961).

FIGURE CAPTIONS

Fig. 1 Schematic section view of the explosive loading assembly and specimen sandwich arrangement.

Fig. 2 Residual shock hardness versus pressure for nickel and Inconel 600 alloy.

Fig. 3 Annealed (unshocked) Inconel microstructure showing coherent precipitate distribution and nominal dislocation density. Sharp coherency strain contours are indicated at "S", while "n" indicates various dislocation dipole nodes. The grain surface normal is tilted off [110].

Fig. 4 Transmission electron micrograph of Inconel residual substructure showing planar dislocation arrays and interaction with precipitates following 50 Kb shock-loading. The grain surface normal is close to [110]. Several dislocation loops and dipoles are recognizable.

Fig. 5 Inconel residual microstructure also following 50 Kb shock for comparison with Fig. 4. A large number of dislocation loops are visible as indicated at "p". The frequency of dipole production can be recognized as specifically noted at "dp". Grain surface normal is close to [110].

Fig. 6 Transmission electron micrograph showing Inconel substructure following 200 Kb shock-loading. Note the profusion of dislocation loops and tangles. The precipitates appear, for the most part, free of coherency strains and the frequency of dislocation dipoles has increased markedly from 50 Kb. The grain surface normal is close to [110].

Fig. 7 Deformation twin structures typical of the residual Inconel substructure following shock-loading at 370 Kb. The twin width was estimated in several instances by measuring the intersection widths for the twins as shown by "i". The grain surface normal is close to [100].

Fig. 8 Dark-field electron micrographs of the respective {111} twin families of Fig. 7 with the objective aperture centered over the twin spots encircled in the superposed selected-area electron diffraction pattern.

(a) Aperture dark-field image using T_1.

(b) Aperture dark-field image using T_2.

Fig. 9 Transmission electron micrograph illustrating the typical residual substructure in nickel shock-loaded at 370 Kb to be dislocation cells. A high density of dislocation loops having an average diameter of 50 $\mathring{A}$ is also visible in the clear regions within the cells. The grain surface normal is close to [110].

Table 1. Sample Composition (weight percent)

Element Composition	Material	
	Nickel	Inconel 600
Ni%	99.970	76.260
Co%	0.010	0.010
Cr%	——	15.910
Fe%	0.004	7.300
Mn%	0.008	0.130
Cu%	0.001	0.020
Si%	0.004	0.280
C%	——	0.060
Al%	0.003	——

Table 2. Residual Defect Densities in Shock-Deformed Inconel

Pressure (Kilobars)	Dislocation Density (cm^{-2})	Deformation Twin Density (volume per cent)
0	2.0×10^{7}	0
50	1.7×10^{10}	0
100	2.0×10^{10}	0
150	2.7×10^{10}	0
200	3.4×10^{10}	0
370	1.5×10^{11}	19

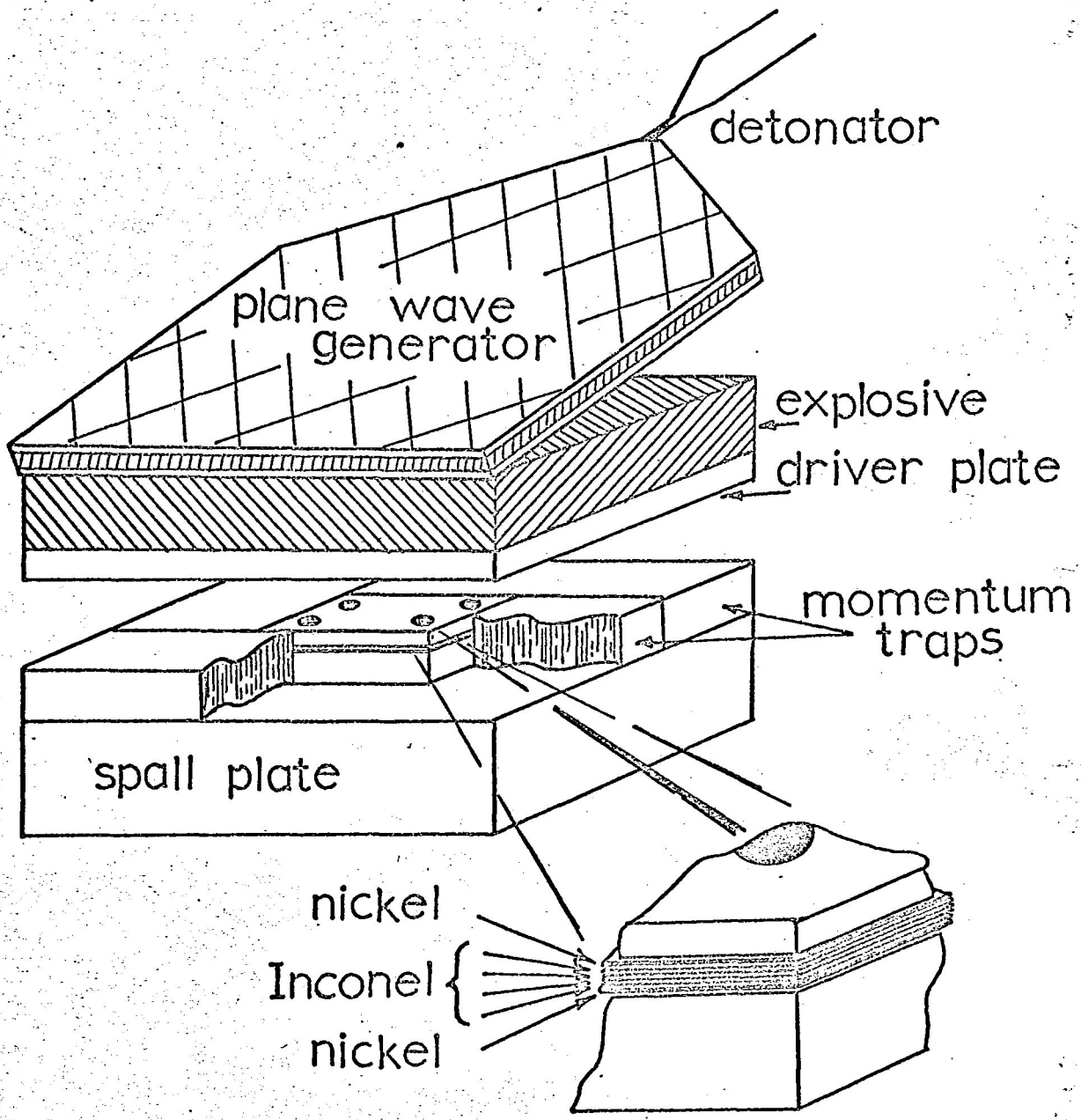

SPECIMEN HOLDER—
enlarged view of sandwiched
specimen sheets

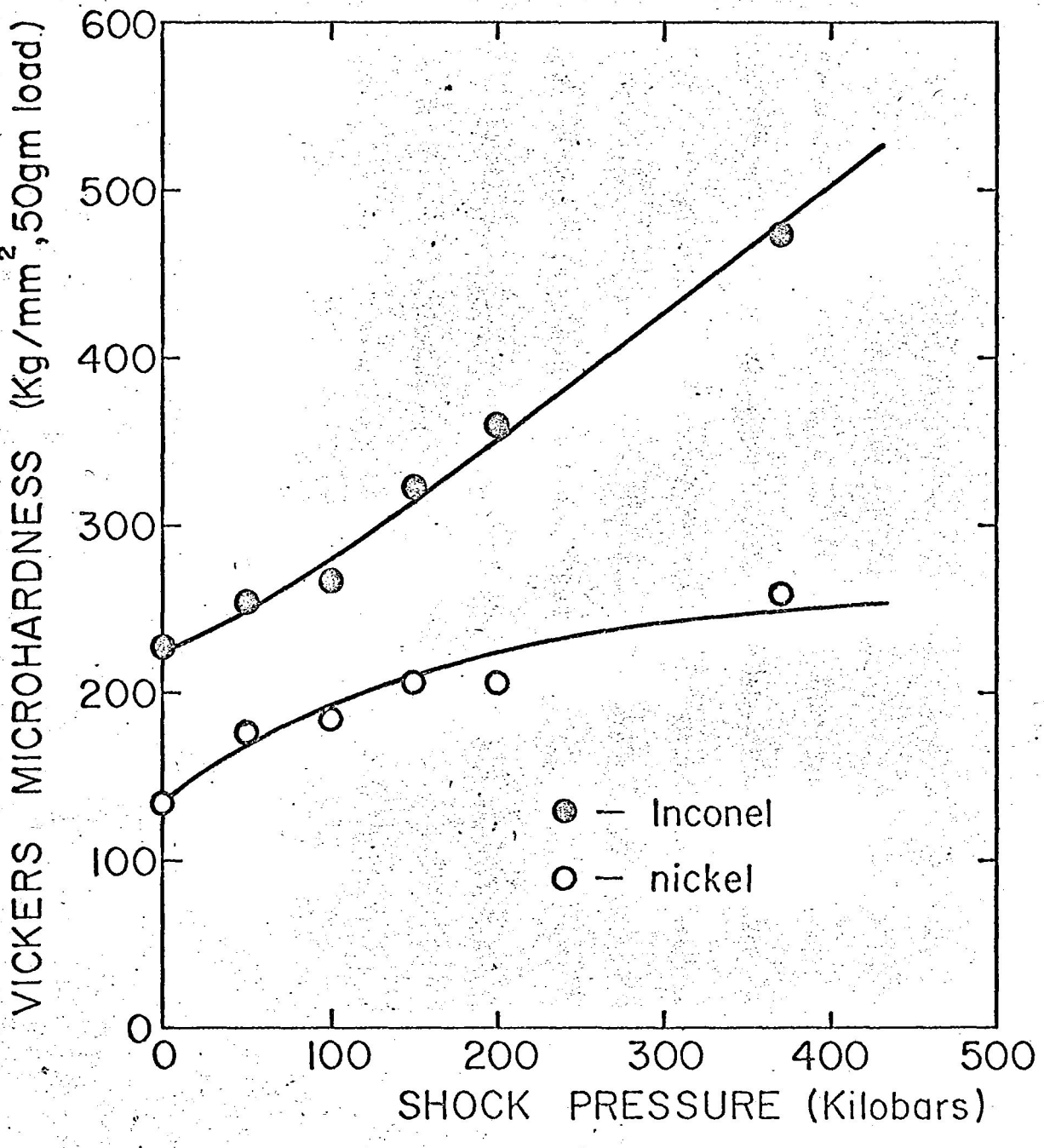
VICKERS MICROHARDNESS (Kg/mm², 50gm load)
600
500
400
300
200
100
0
0
100
200
300
400
500
SHOCK PRESSURE (Kilobars)
— Inconel
— nickel

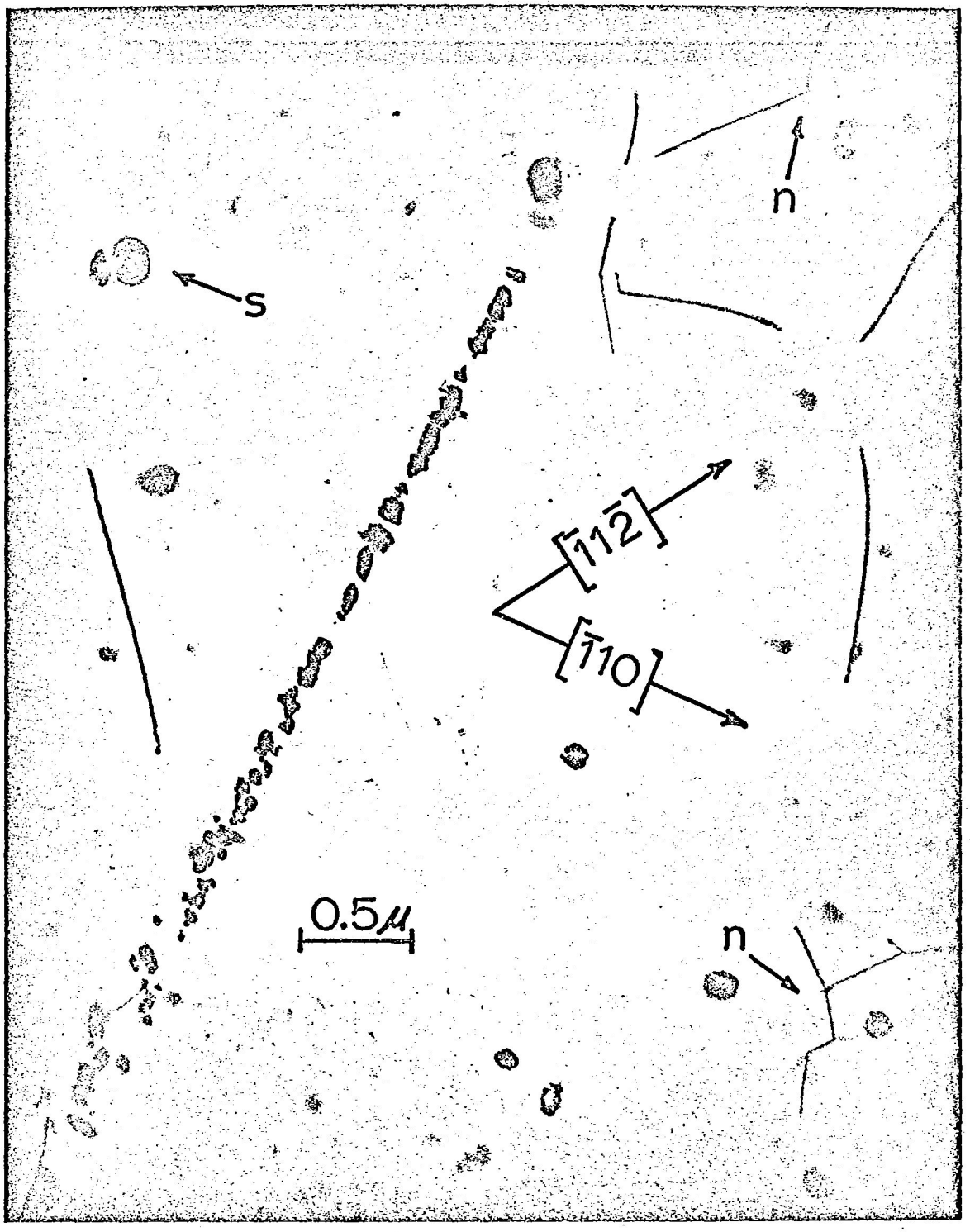
n
s
[11$\bar{2}$]
[$\bar{1}$10]
0.5μ
n

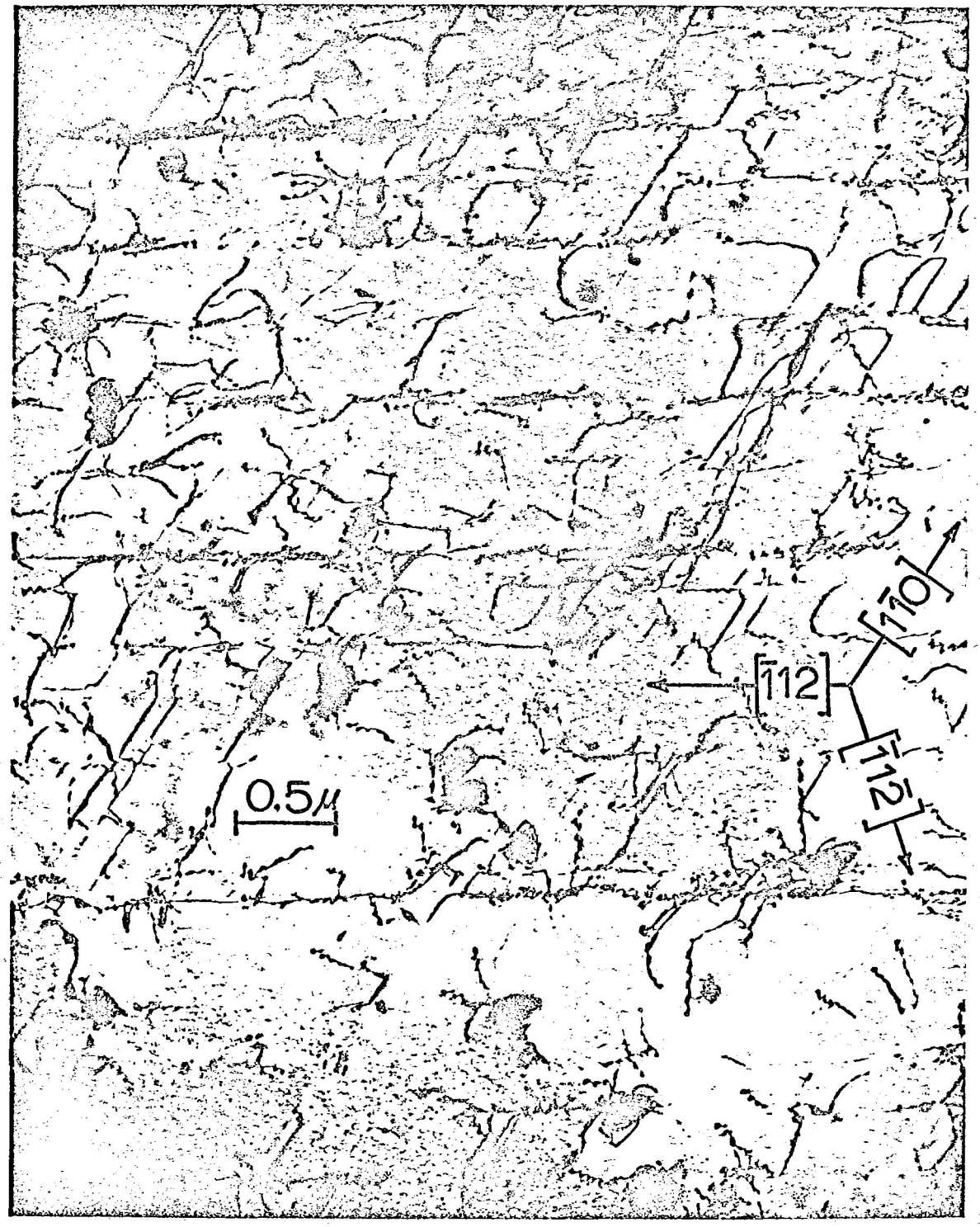
[1$\bar{1}$0]
[112]
[$\bar{1}$12]
0.5μ

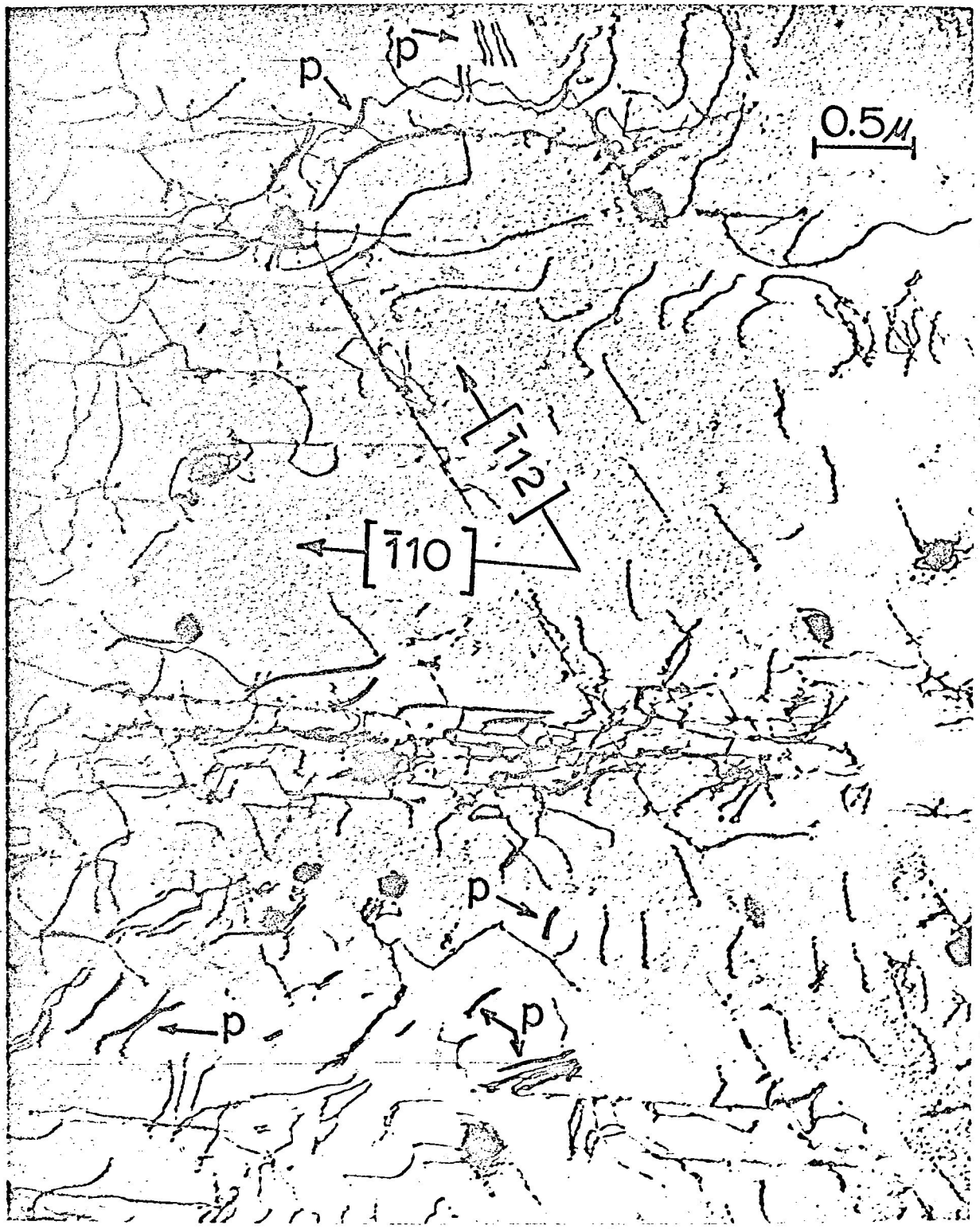
p
p
0.5μ
[112]
[1̄10]
p
p
p

0.5μ
[1$\bar{1}$0]
[11$\bar{2}$]
[$\bar{1}$12]

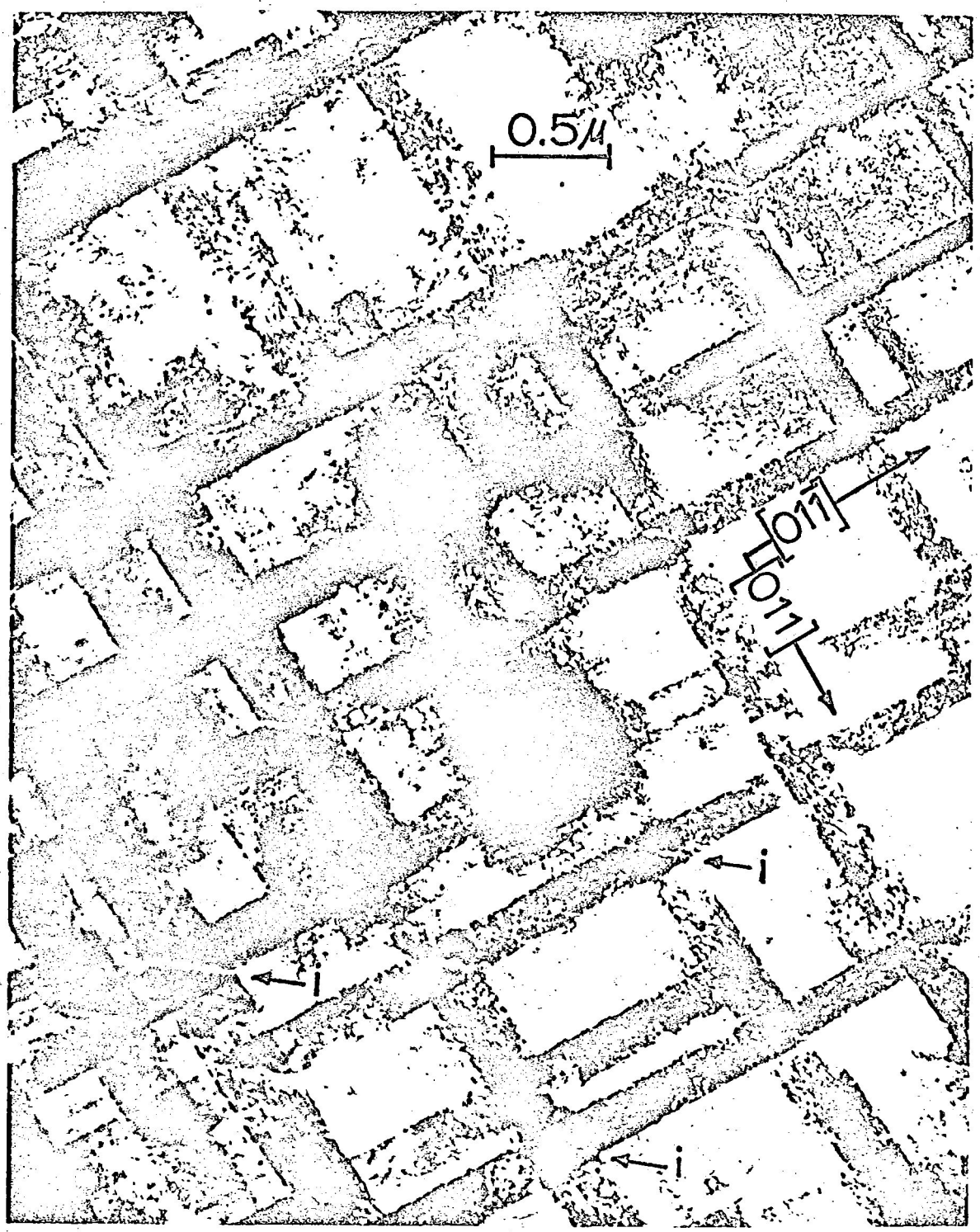
0.5μ
[011]
[110]
i
i
i

8 T1
T2
0.5μ

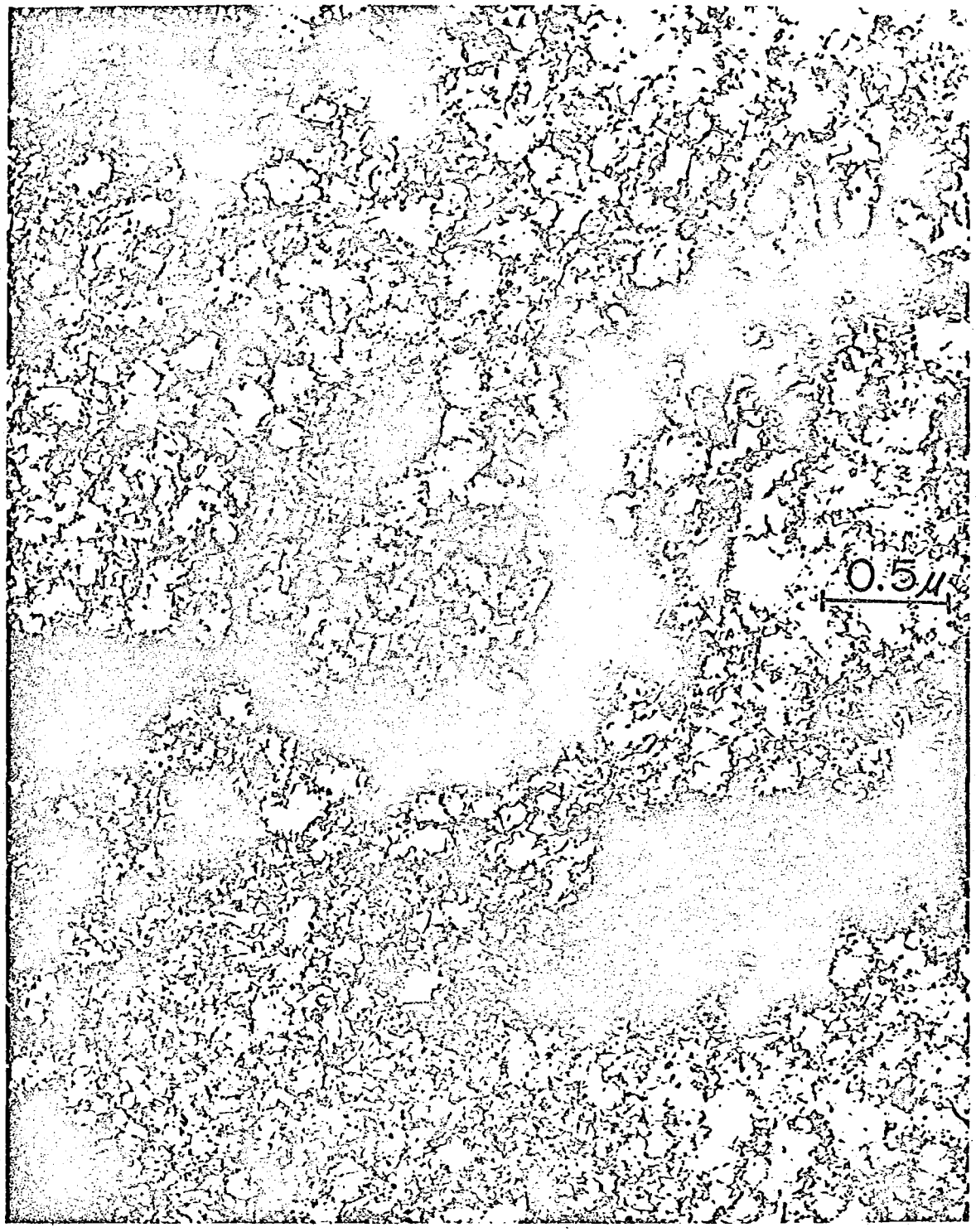
0.5μ